NASA TECHNICAL MEMORANDUM

NASA TM X-71649

NASA TM X- 71649

(NASA-TM-X-71649) NUMERICAL EVALUATION OF THE SURFACE DEFORMATION OF ELASTIC SOLIDS SUBJECTED TO A HERTZIAN CONTACT STRESS (NASA) 8 p HC $3.25 CSCL 20K G3/39

N75-16016

Unclas 07775

NUMERICAL EVALUATION OF THE SURFACE DEFORMATION OF ELASTIC SOLIDS SUBJECTED TO A HERTZIAN CONTACT STRESS

by D. Dowson and B. J. Hamrock
Lewis Research Center
Cleveland, Ohio 44135

FEB 1975
NASA STI FACILITY
INPUT BRANCH

TECHNICAL PAPER to be presented at
International Lubrication Conference cosponsored
by the Japanese Society of Lubrication Engineers
and the American Society of Lubrication Engineers
Tokyo, Japan, June 9-11, 1975

Numerical Evaluation of the Surface Deformation of Elastic Solids Subjected to a Hertzian Contact Stress

D. Dowson[1] B. J. Hamrock[2]

The elastic deformation of two ellipsoidal solids in contact and subjected to a Hertzian stress distribution has been evaluated numerically as part of a general study of the elastic deformation of such solids in elastohydrodynamic contacts. In the analysis the contact zone is divided into equal rectangular areas and it is assumed that a uniform pressure is applied over each rectangular area. A study has been made of the influence on the size of the rectangular area upon accuracy. The results also indicate how far from the center of the contact one needs to go before elastic deformation becomes insignificant.

E-7964

SYMBOLS

a = Semimajor axis of contact ellipse

$\bar{a}$ = $a/2m$

b = Semiminor axis of contact ellipse

$\bar{b}$ = $b/2m$

D = Defined by eq. (2)

E = Modulus of elasticity

$$E' = 2\Big/\left\{\left[\left(1-\nu_A^2\right)\Big/E_A\right]+\left[\left(1-\nu_B^2\right)\Big/E_B\right]\right\}$$

F = Normal applied force

h = Total film thickness

h_o = Central film thickness due to elastohydrodynamic lubrication

m = Number of divisions of the semimajor or semiminir axis

P = p/E', dimensionless pressure

p = Pressure

R = Effective radius

R_2 = w/S

$R_3 = 100\left[(w_m - w_{3m})/w_{3m}\right]$

$\bar{r}$ = Defined in fig. 3

S = Film thickness due to the geometry of the solids, defined in eq. (8)

W = $F/E'R_xR_y$, dimensionless load parameter

w = Total elastic deformation

$\bar{w}$ = Elastic deformation

$X_1, X, \bar{X}, x$ } = Coordinate systems defined in the
$Y_1, Y, \bar{Y}, y$ } = paper

ν = Poisson's ratio

Subscripts:

A = Refers to solid A

B = Refers to solid B

x, y = Refers to the coordinate system defined in the paper

INTRODUCTION

Elastohydrodynamic lubrication (ref. 1) is defined as the study of situations in which elastic deformation of the surrounding solids plays a sig-

[1]Professor, Dept. of Mechanical Engineering, Leeds Univ., Leeds, England.

[2]Bearing Analyst, NASA Lewis Research Center, Cleveland, Ohio, U.S.A.

nificant role in the hydrodynamic lubrication process. This paper will not be concerned with the hydrodynamic lubrication process but only with the deformation due to pressure of one elastic solid upon another. Succeeding papers will deal with the coupling of the elastic deformation and hydrodynamic equations with the object of obtaining a complete three-dimensional pressure and film thickness profile. Reference 1 distinguishes between two forms of distortions which may exist in machine elements. The contact geometry may be affected by overall distortion of the elastic machine element resulting from applied loads as shown in figure 1(a).

In addition the normal stress distribution in the vicinity of the contact may produce local elastic deformations which are significant when compared with the lubricant film thickness, as shown in figure 1(b). This is the mode of deformation with which this report will concern itself. The important distinction is that the first form of deformation is relatively insensitive to the distribution and magnitude of the stresses in the contact zone, whereas the second mode of deformation is intimately linked to the local stress conditions.

The deformation analysis will assume that the contact can be divided into rectangular areas and that the pressure can be assumed to be uniform within each rectangular area. Once the elastic deformation has been formulated, investigations will be performed to answer the following queries:

(1) How fine do the semimajor and semiminor axes need to be divided to achieve a given accuracy in deformation prediction?

(2) How far out from the center of the contact is it necessary to go before deformation becomes insignificant compared with the natural separation of the solids?

These questions will be investigated for light and heavy applied loads, for equal spheres in contact, and for a contact that is common to the outer race of a ball bearing. The results of this investigation are given in greater detail in reference 2.

GEOMETRY OF CONTACTING ELASTIC SOLIDS

Two solids having different radii of curvature in a pair of principal planes (x and y) passing through the contact between the solids make contact at a single point under the condition of no applied load. Such a condition is called point contact and is shown in figure 2. Now when the two solids in figure 2 have a normal load applied to them, the result is that the point expands to an ellipse with "a" being the semimajor axis and "b" being the semiminor axis. The normal applied load "F" in figure 2 lies along the axis which passes through the center of the solids and through the point of the contact and is perpendicular to a plane which is tangential to both solids at the point of contact. The method used in evaluating the semimajor and semiminor axes is the same as that used in reference 3 and therefore will not be repeated here.

ELASTIC DEFORMATION

Having the semimajor and semiminor axis of the contact ellipse the elastic deformation which occurs inside and outside the contact can be evaluated. The approach to be used here will be one that can be quickly evaluated on the digital computer. The reason for this is that succeeding papers will deal with coupling the elastic deformation with hydrodynamic equations thereby complicating things considerably. Therefore an elastic deformation analysis that is quickly evaluated and accurate will help assure success of succeeding papers of elastohydrodynamic lubrication of point contacts. Figure 3 shows a rectangular area of uniform pressure with the coordinate system to be used. From Timoshenko and Goodier (ref. 4) the elastic deformation at a point (X, Y) of a semi-infinite solid subjected to a pressure "p" at the point (X_1, Y_1) can be written as

$$d\bar{w} = \frac{2p\, dX_1\, dY_1}{\pi E' \bar{r}}$$

The elastic deformation at a point (X, Y) due to the uniform pressure over the rectangular area $2\bar{a} \times 2\bar{b}$ is thus

$$\bar{w} = \frac{2P}{\pi} \int_{-\bar{a}}^{\bar{a}} \int_{-\bar{b}}^{\bar{b}} \frac{dX_1\, dY_1}{\sqrt{(Y - Y_1)^2 + (X - X_1)^2}}$$

where

$$P = \frac{p}{E'}$$

Integrating the above gives

$$\bar{w} = \frac{2}{\pi} PD \tag{1}$$

where

$$D = (X+b)\ln\left[\frac{(Y+\bar{a}) + \sqrt{(Y+\bar{a})^2 + (X+\bar{b})^2}}{(Y-\bar{a}) + \sqrt{(Y-\bar{a})^2 + (X+\bar{b})^2}}\right]$$

$$+ (Y+a)\ln\left[\frac{(X+\bar{b}) + \sqrt{(Y+\bar{a})^2 + (X+\bar{b})^2}}{(X-\bar{b}) + \sqrt{(Y+\bar{a})^2 + (X-\bar{b})^2}}\right]$$

$$+ (X-b)\ln\left[\frac{(Y-\bar{a}) + \sqrt{(Y-\bar{a})^2 + (X-\bar{b})^2}}{(Y+\bar{a}) + \sqrt{(Y+\bar{a})^2 + (X-\bar{b})^2}}\right]$$

$$+ (Y-a)\ln\left[\frac{(X-\bar{b}) + \sqrt{(Y-\bar{a})^2 + (X-\bar{b})^2}}{(X+\bar{b}) + \sqrt{(Y-\bar{a})^2 + (X+\bar{b})^2}}\right] \tag{2}$$

Now "$\bar{w}$" in equation (1) represents the elastic deformation at a point (X, Y) due to a rectangular area ($2\bar{a} \times 2\bar{b}$) of uniform pressure "p." If the contact ellipse is divided into a number of equal rectangular areas, the total deformation at a point (X, Y) due to the contributions of the various rectangular areas of uniform pressure in the contact ellipse can be evaluated numerically. Figure 4 shows a sample of dividing the area inside and outside the contact into a number of equal rectangular areas. For purposes of illustration the contact was divided into a grid of 6 × 6 rectangular areas. The effect of the fineness of this grid will be discussed later. Making use of figure 4 the total elastic deformation at any point inside or outside the contact ellipse due to the rectangular areas of uniform pressure within the contact can be written as

$$w_{k,\ell} = \frac{2}{\pi} \sum_{j=1,\ldots}^{6} \sum_{i=1,\ldots}^{6} P_{i,j} D_{m,n} \tag{3}$$

where

$$m = |k - i + 1| \tag{4}$$

$$n = |\ell - j + 1| \tag{5}$$

PRESSURE DISTRIBUTION

Within the contact ellipse the pressure will be assumed to be Hertzian. Therefore, using the coordinate system of figure 4 the dimensionless pressure is

$$P = \frac{3wR_xR_y}{2\pi ab}\sqrt{1 - \left(\frac{\bar{Y} - a}{a}\right)^2 - \left(\frac{\bar{X} - b}{b}\right)^2} \tag{6}$$

where

$$W = \frac{F}{E'R_xR_y} \tag{7}$$

$$\frac{1}{R_x} = \frac{1}{r_{Ax}} + \frac{1}{r_{Bx}}$$

$$\frac{1}{R_y} = \frac{1}{r_{Ay}} + \frac{1}{r_{By}}$$

The pressure outside the contact will be assumed to be zero.

FILM THICKNESS

The distance separating the two undistorted solids shown in figure 2 while using the coordinate system developed in figure 4 can be written as

$$S = \frac{(\bar{X} - b)^2}{2R_x} + \frac{(\bar{Y} - a)^2}{2R_y} \tag{8}$$

The total film thickness when a contact is elastohydrodynamically lubricated can be written as

$$h = h_o + S(\bar{X}, \bar{Y}) + w(\bar{X}, \bar{Y}) \tag{9}$$

where

h_o central film thickness due to elastohydrodynamic lubrication

w elastic deformation inside and outside the contact region

The significance of the elastic deformation relative to the film thickness due to the geometry of the contacting solids can be expressed as

$$R_2 = \frac{w}{S} \tag{10}$$

INPUT CONDITIONS

From figure 4 it can be seen that we need to concern ourselves with the following:

(1) How fine must the divisions of "a" and "b" be? We will assume that the number of divisions of "a" and "b" will be the same. Therefore,

$$m = \frac{a}{2\bar{a}} = \frac{b}{2\bar{b}} \tag{11}$$

In this paper we will let m = 3, 4, and 5.

(2) How far from the semimajor and semiminor axes must one go before R_2 (eq. (10)) becomes insignificant?

To check the accuracy of the elastic deformation results for m = 3, 4, and 5 the number of equal divisions along the semimajor and semiminor axes are increased by three times (m = 9, 12, and 15) and then corresponding points are compared. The following equation describes the percentage accuracy of the results compared with the finest mesh size predictions.

$$R_3 = \left(\frac{w_m - w_{3m}}{w_{3m}}\right)100 \tag{12}$$

The limiting conditions that were evaluated on the computer are shown in table I. It was speculated that conclusions which could be made for these limiting conditions could also be made for any intermediate conditions. The four limiting conditions shown in table I are two extremes of applied normal load, a light load of 8.964 N (2 lb) and a heavy load of 896.4 N (200 lb). The two extremes of curvature of the solids shown in table I are equal spheres in contact and a ball and outer race of a ball bearing. The elliptical eccentricity parameter (k = a/b) for the equal spheres in contact is equal to one and for the ball and outer ract it is equal to five.

DISCUSSION OF RESULTS

Tables II and III give the characteristics of the deformed shape of the contacting solids along the semimajor and semiminor axes when the axes are divided into five equal divisions and the dimensionless load parameter is equated to 0.2102×10^{-7} and 0.2102×10^{-5}. Some observations which can be made about these tables are:

(1) Comparing table II with III, which amounts to changing the normal applied load from 8.964 N (2 lb) to 896.4 N (200 lb), the following can be concluded:

(a) R_2 does not change in the corresponding tables. That is, regardless of the normal applied load, the ratio of the elastic deformation to the natural separation of the solids is unchanged.

(b) R_3 does not change in the corresponding tables. This condition is no doubt because of the condition mentioned in 1(a).

(2) The separation due to the geometry of the contacting solids plus the elastic deformation (S + w) is very close to being constant in the contact. The value of (S + w) at the farthest point from the center of the contact and yet still in the contact differs the most from the other values of (S + w) in the contact, increasing slightly.

(3) The percentabe difference in surface deformation calculations for two mesh sizes differing by a factor of three was shown to be small. For the worst case R_3 was found to be less than 2 percent. That is the elastic deformation for m = 5 at corresponding points and m = 15 differ by less than 2 percent, which is extremely good.

(4) The ratio of the elastic deformation to the natural separation of the contacting solids, R_2, is seen to decrease substantially as one moves away from the center of the contact.

In order to better illustrate the results shown in the tables, figures 5 through 9 are presented. In figures 5 through 8 the solid curve represents the case of equal spheres in contact which is represented by $R_x = R_y = 0.558$ centimeter (0.2188 in.) and the dotted curve represents the ball and outer race in contact which is represented by $R_x = 1.284$ centimeters (0.5055 in.), $R_y = 15.00$ centimeters (5.906 in.). Also due to the observation made in discussing the tables that R_2 and R_3 are not a function of the normal applied load the results shown in figures 5 through 8 apply for any normal applied load.

Figure 5 shows the effects of the location along the semimajor axis on the percentage difference in elastic deformation when $m = 3$ and $m = 9$. Here an "edge effect" can be seen which is a rapid rise in percentage difference in the elastic deformation when $m = 3$ and for corresponding points when $m = 9$. This rapid rise is due to the pressure being either zero if the center of the rectangular area shown in figure 4 is outside the contact or of order 10^5 if the center of the rectangular area is within the contact. However, it is speculated that in lubricated contacts where the pressure gradients are, in general, more gradual than those encountered near the edge of a dry Hertzian contact, this "edge effect" is likely to be less significant. It is also to be noted in figure 5 that outside the contact, the value of R_3 decreases rapidly.

Figure 6 shows the effect of the location along the semimajor axis on the percentage difference in elastic deformation when $m = 3$, 4, and 5 and the more exact elastic deformation when $m = 9$, 12, and 15, respectively. In this figure we see a large drop in R_3 when going from $m = 4$ to $m = 5$. This also brings down the edge effect considerably. This therefore, makes a good case for letting $m = 5$ in any further computer evaluations.

Figures 7 and 8 show the effect on the location along the semimajor and semiminor axes on the ratio of the elastic deformation to the distance separating the two solids in contact due to the geometry of the solids. Here we see the difference that the shape of the contact has on how far from the semimajor and semiminor axes one needs to go before the elastic deformation becomes insignificant. To be more specific, from the curves we see that for equal spheres in contact (represented by solid lines in the figures) $R_2 < 0.05$ corresponds to $x > 2.6\,b$ and $y > 2.6\,a$. This means that the elastic deformation is less than 5 percent of the film thickness due to the geometry effects when one moves away from the center of the contact a distance no less than 2.6 times the semimajor or semiminor axes. For the ball and outer race in contact $R_2 < 0.05$ correspond to $y \geq 1.9\,a$ and $x \geq 4.0\,b$. This means that the elastic deformation is less than 5 percent of the film shape due to geometry effects when one moves only 1.9 times the semimajor axis away from the center of the contact and 4.0 times the semiminor axis from the center of the contact.

Figure 9 shows the effect of the location along the semimajor axis on the separation due to the geometry of the contacting solids plus the elastic deformation $(S + w)$ when the dimensionless load parameter is 0.2107×10^{-7}, 0.5105×10^{-7}, 0.2107×10^{-5}, and 0.5105×10^{-5}. This figure shows that $(S + w)$ is constant within the contact.

CONCLUSIONS

A numerical analysis of the surface deformation of two contacting ellipsoidal solids has been performed. The analysis assumed that the pressure in the contact was Hertzian. It was assumed that the contact could be divided into rectangular areas with the pressure assumed to be uniform within each rectangular area. The resulting equations were programmed on a digital computer. Four limiting conditions were evaluated on the computer. They consist of two extremes of applied normal loads, a light load of 8.964 N (2 lb) and a heavy load of 896.4 N (200 lb). The two other extremes are of the curvature of the contacting solids. One of them is two equal spheres in contact and the other is that of a ball and outer race of a ball bearing. It was speculated that conclusions which could be made for the limiting conditions could also be made for any intermediate conditions.

The results indicate that division of the semimajor and semiminor axes into five equal subdivisions is adequate to obtain accurate elastic deformation results. It was also found that the elastic deformation becomes insignificant compared with the normal surface separation for two equal spheres in contact at a distance from the center of 2.6 times the semimajor axis. For a ball and outer race in contact it was found that a similar observation applied at a distance from the center of 1.9 times the semimajor axis and 4.0 times the semiminor axis. Finally, it was found that the separation due to the geometry of the contacting solids plus the elastic deformation $(S + w)$ was almost constant in the contact region. However, numerical values of $(S + w)$ at points near the edge

of the Hertzian contact show that a slight "edge effect" or error may be encountered in such regions. In lubricated contacts where the pressure gradients are, in general, more gradual than those encountered near the edge of a dry Hertzian contact, this effect is likely to be less significant.

REFERENCES

(1) Dowson, D., "Elastohydrodynamic Lubrication - An Introduction and a Review of Theoretical Studies", Symposium on Elastohydrodynamic Lubrication, 1965, Leeds, England.

(2) Hamrock, B. J., and Dowson, D., "Numerical Evaluation of the Surface Deformation of Elastic Solids Subjected to a Hertzian Contact Stress", NASA TN D-7774, 1974.

(3) Hamrock, B. J., and Anderson, W. J., "Analysis of an Arched Outer-Race Ball Bearing Considering Centrifugal Forces", Journal of Lubrication Technology, Trans. ASME, Series F, Vol. 95, No. 3, Jul. 1973, pp. 265-276.

(4) Timoshenko, S., and Goodier, J. N., Theory of Elasticity, 2nd ed., McGraw-Hill Book Co., Inc., 1951.

TABLE I. - INPUT CONDITIONS USED FOR COMPUTER EVALUATIONS

[Effective elastic modulus, E', 21.97 MN/cm^2 (3.187×10^7 psi); radius of curvature for solid A, $r_{Ax} = r_{Ay} = 1.111$ cm (0.4375 in.).]

Condition	Dimensionless load parameter, W	Normal applied force, F		Effective radius R_x		R_y		Radius of curvature for solid B r_{Bx}		r_{By}	
		N	lbf	cm	in.	cm	in.	cm	in.	cm	in.
1	0.5105×10^{-7}	8.964	2	0.5556	0.2188	0.5556	0.2188	1.111	0.4375	1.111	0.4375
2	$.5105\times10^{-5}$	896.4	200	.5556	.2188	.5556	.2188	1.111	.4375	1.111	.4375
3	$.2102\times10^{-7}$	8.964	2	1.284	.5055	15.00	5.906	-8.260	-3.252	-1.200	-.4725
4	$.2102\times10^{-5}$	896.4	200	1.284	.5055	15.00	5.906	-8.260	-3.252	-1.200	-.4725

TABLE II. - CHARACTERISTICS OF THE FILM SHAPE ALONG THE SEMIMAJOR AND SEMIMINOR AXIS

Coordinates $\bar{X}$	Coordinates $\bar{Y}$	Pressure, p, N/cm^2	Elastic deformation, w, cm	Ratio $R_2 = \frac{w}{S}$	Total separation, S + w, cm	Ratio R_3
11b̄	11ā	0.0253×10^6	0.0401×10^{-3}	99.24	0.0406×10^{-3}	0.1962
	13ā	.0243	.0378	14.58	.0406	.1273
	15ā	.0220	.0335	4.786	.0404	.0682
	17ā	.0181	.0269	1.981	.0406	.0094
	19ā	.0108	.0185	.8242	.0409	1.621
	21ā	0	.0107	.3220	.0442	------
	23ā	|	.0081	.1749	.0546	------
	25ā	|	.0066	.1085	.0688	------
	27ā	|	.0058	.0725	.0853	------
	29ā	|	.0052	.0510	.1044	------
	31ā	|	.0046	.0373	.1257	------
	33ā	|	.0041	.0282	.1496	------
	35ā	|	.0038	.0218	.1755	------
	37ā	|	.0036	.0172	.2040	------
	39ā	|	.0033	.0138	.2344	------
	41ā	|	.0030	.0113	.2672	------
	43ā	|	.0028	.0093	.3023	------
	45ā	|	.0025	.0078	.3393	------
	47ā	|	.0025	.0066	.3787	------
	49ā	↓	.0023	.0055	.4204	------
13b̄	11ā	.0243	.0391	27.05	.0406	.2210
15b̄		.0220	.0371	10.50	.0406	.2814
17b̄		.0181	.0340	5.105	.0406	.4123
19b̄		.0108	.0300	2.767	.0409	.6459
21b̄		0	.0257	1.597	.0417	------
23b̄		|	.0229	1.025	.0452	------
25b̄		|	.0208	.7020	.0503	------
27b̄		|	.0191	.5036	.0512	------
29b̄		|	.0176	.3742	.0650	------
31b̄		|	.0165	.2859	.0744	------
33b̄		|	.0155	.2235	.0848	------
35b̄		|	.0145	.1781	.0963	------
37b̄		|	.0137	.1442	.1090	------
39b̄		|	.0130	.1184	.1229	------
41b̄		|	.0124	.0984	.1379	------
43b̄		|	.0117	.0827	.1589	------
45b̄		|	.0112	.0702	.1712	------
47b̄		|	.0101	.0600	.1895	------
49b̄		↓	.0102	.0517	.2088	------

TABLE III. - CHARACTERISTICS OF THE FILM SHAPE ALONG THE SEMIMAJOR AND SEMIMINOR AXES

Coordinates $\bar{X}$	Coordinates $\bar{Y}$	Pressure p, N/cm^2	Ratio $R_1 = \frac{S}{S}$	Elastic deformation, w, cm	Ratio $R_2 = \frac{w}{S}$	Total separation, S + w, cm	Ratio R_3
11b̄	11ā	0.1179×10^6	1.000	0.8661×10^{-3}	99.24	0.8750×10^{-3}	0.1998
	13ā	.1126	|	.8179	14.58	.8740	.1244
	15ā	.1021	|	.7216	4.786	.8725	.0668
	17ā	.0839	|	.5804	1.981	.8733	.0088
	19ā	.0503	|	.3975	.8242	.8799	1.617
	21ā	0	|	.2316	.3220	.9501	------
	23ā	|	|	.1755	.1749	1.179	------
	25ā	|	↓	.1448	.1085	1.480	------
	27ā	|	.9999	.1242	.0725	1.838	------
	29ā	|	|	.1092	.0510	2.249	------
	31ā	|	|	.0975	.0373	2.710	------
	33ā	|	|	.0884	.0282	3.223	------
	35ā	|	|	.0808	.0218	3.785	------
	37ā	|	↓	.0744	.0172	4.392	------
	39ā	|	.9998	.0688	.0138	5.050	------
	41ā	|	|	.0643	.0113	5.756	------
	43ā	|	|	.0602	.0093	6.510	------
	45ā	|	|	.0566	.0078	7.310	------
	47ā	|	.9997	.0536	.0066	8.161	------
	49ā	↓	↓	.0508	.0056	9.058	------
13b̄	11ā	.1126	1.000	.8440	27.05	.8753	.2262
15b̄		.1021	1.000	.7996	10.50	.8755	.2836
17b̄		.0839	1.000	.7330	5.105	.8766	.4141
19b̄		.0503	.9999	.6459	2.767	.8793	.6447
21b̄		0	.9999	.5525	1.597	.8981	------
23b̄		|	.9998	.4925	1.025	.9731	------
25b̄		|	.9998	.4478	.7020	1.036	------
27b̄		|	.9997	.4117	.5036	1.230	------
29b̄		|	.9996	.3818	.3742	1.402	------
31b̄		|	.9995	.3559	.2859	1.601	------
33b̄		|	.9994	.3335	.2235	1.825	------
35b̄		|	.9993	.3137	.1781	2.075	------
37b̄		|	.9992	.2962	.1442	2.350	------
39b̄		|	.9991	.2804	.1184	2.649	------
41b̄		|	.9990	.2664	.0984	2.972	------
43b̄		|	.9988	.2535	.0827	3.320	------
45b̄		|	.9987	.2418	.0702	3.688	------
47b̄		|	.9985	.2311	.0600	4.082	------
49b̄		↓	.9983	.2212	.0517	4.501	------

ORIGINAL PAGE IS OF POOR QUALITY

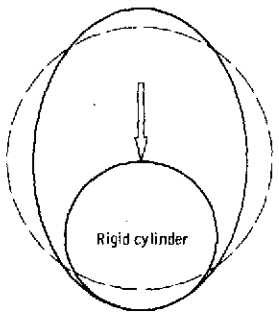

(a) Distortion of the element.

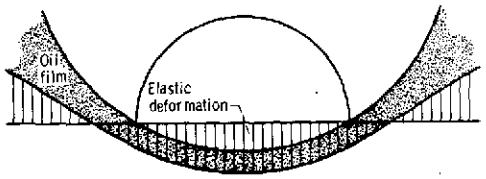

(b) Local elastic deformation.

Figure 1. - Types of elastic deformation.

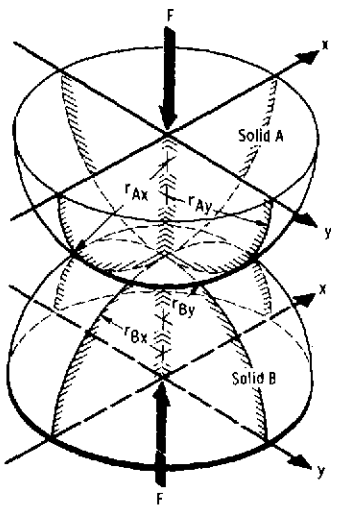

Figure 2. - Geometry of contacting elastic solids.

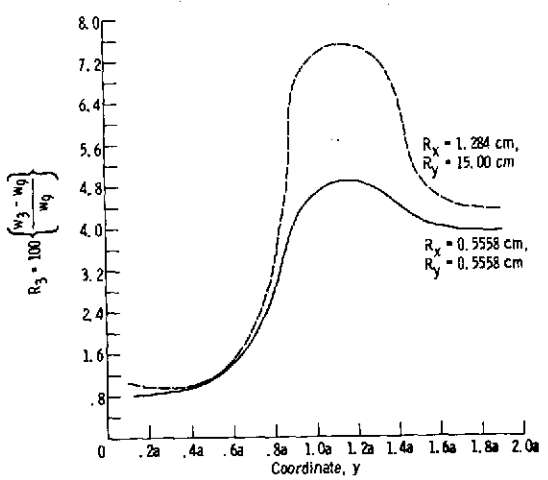

Figure 5. - Effect of location along the semimajor axis on the percentage difference in elastic deformation when m = 3 and when m = 9.

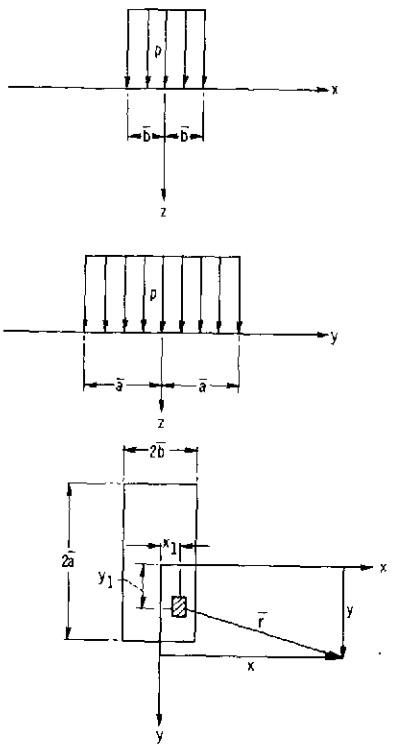

Figure 3. - Surface deformation of a semi-infinite body subjected to a uniform pressure over a rectangular area.

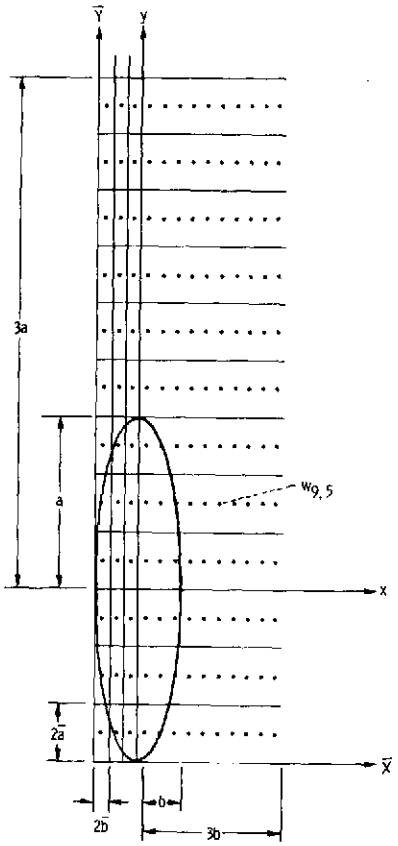

Figure 4. - Sample of how the area in and around the contact may be divided into equal rectangular areas.

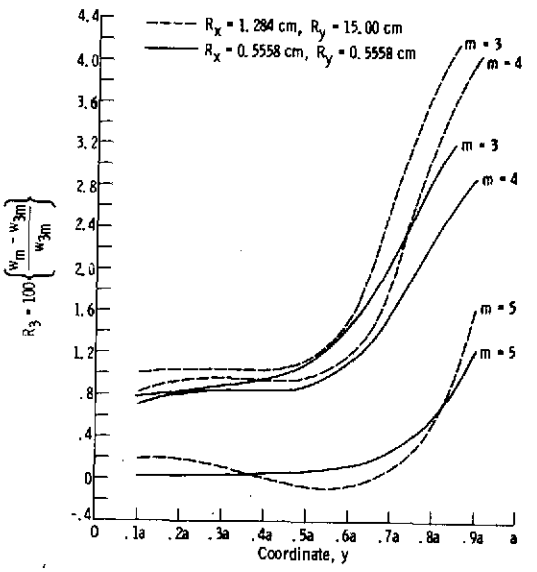

Figure 6. - Effect of location along the semimajor axis on the percentage difference in the elastic deformation when m = 3, 4 and 5 and the more exact film shape when m = 9, 12 and 15, respectively.

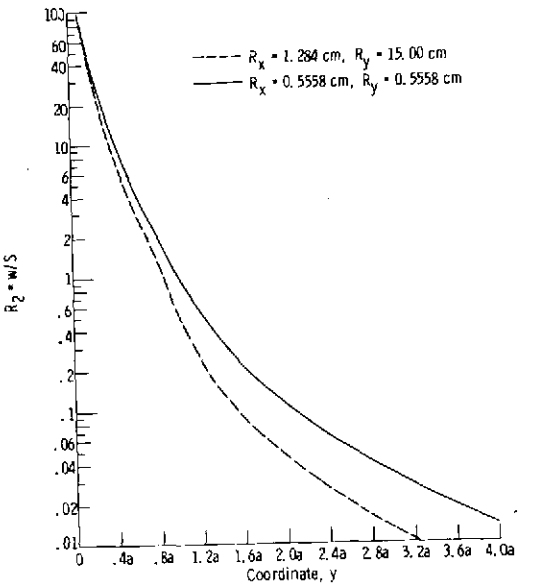

Figure 7. - Effect of the location along the semimajor axis on the ratio of the elastic deformation to the distance separating the two solids in contact due to the geometry of the solids for m = 5.

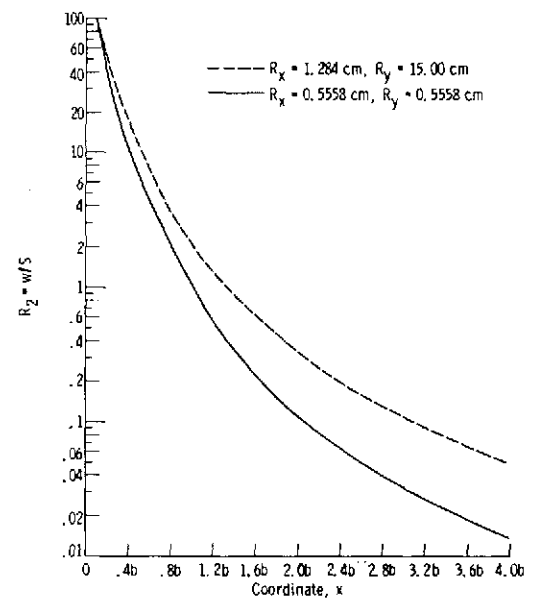

Figure 8. - Effect of the location along the semiminor axis on the ratio of the elastic deformation to the distance separating the two solids in contact due to the geometry of the solids for m = 5.

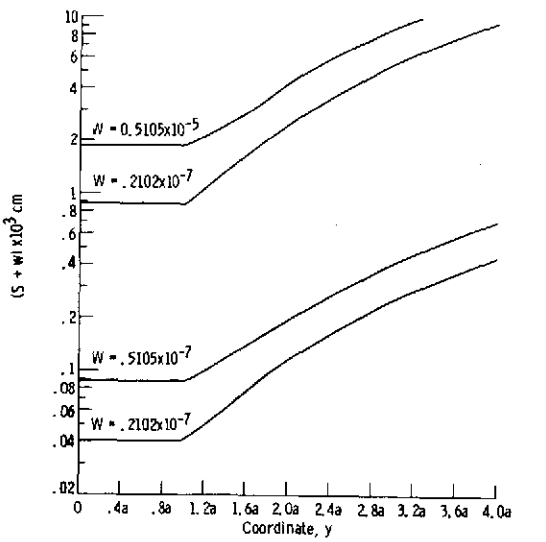

Figure 9. - Effect of the location along the semimajor axis on the separation due to the geometry of the contacting solids plus the elastic deformation for m = 5.